Multi-echo Acquisition of 3D TOF and SWI of Radiation-induced Cerebral Microbleeds at 7T

Wei Bian[1,2], Suchandrima Banerjee[3], Douglas A.C. Kelly[4], Susan M Chang[5], Sarah J Nelson[1,2], and Janine M Lupo[2]

[1]*Graduate Program in Bioengineering, University of California San Francisco & Berkeley, San Francisco, CA, United States,* [2]*Radiology and Biomedical Imaging, University of California San Francisco, San Francisco, CA, United States,* [3]*Global Applied Science Laboratory, GE Healthcare, Menlo Park, CA, United States,* [4]*Global Applied Science Laboratory, GE Healthcare, San Francisco, CA, United States,* [5]*Neurological Surgery, University of California San Francisco, San Francisco, CA, United States*

Introduction: Radiation treatment for brain tumors eventually results in the formation of cerebral microbleeds (CMBs) in otherwise normal appearing brain tissue[1]. While the utility of susceptibility-weighted imaging (SWI) for characterizing both CMBs and intracranial veins and 3D time-of-flight (TOF) MR angiography for visualizing intracranial arteries has been demonstrated throughout the literature[2-3] , these sequences can take up to 20 minutes of combined scan time and are difficult to accurately co-register due to the minimal anatomical contrast required. The ability to obtain a simultaneous acquisition of 3D TOF and SWI in a single imaging sequence with multi-echoes has been recently demonstrated in normal volunteers at 3T[4-5]. The goal of this study was to determine a set of acquisition parameters and reconstruction methods that would result in high-resolution vascular images for the simultaneous depiction of arteries, veins, and CMBs at 7T. We hypothesize that implementation of this technique at 7T will improve image quality due to elevated SNR, better background suppression for TOF, and heightened susceptibility contrast, aiding in CMB detection.

Table 1. CNR calculated for different acquisitions

TOF		SWI				
Single-echo	Multi-echo	Single-echo	Multi-echo (combined)	Multi-echo 2	Multi-echo 3	Multi-echo 4
72.8	61.9	24.6	15.1	10.3	10.3	9.1

* CNR on TOF between background tissue and arteries
* CNR on SWI between white matter and veins

Methods: *Sequence Design:* A multi-echo sequence was created from a single-echo, multi-slab 3D SPGR sequence with TOF capabilities on a GE system by adding 3 additional echoes. The first echo was used to create TOF-MRA images, while the remaining 3 echoes were utilized to generate an SWI image. To minimize the TE of the first echo and overall TR, flow compensation was performed only in readout direction and all echoes were partially acquired with a 65% sampling coverage, resulting in a TE1/TE2/TE3/TE4 of 3.2/9.7/16.2/22.7ms and a TR of 42ms when using a BW of 31.25 kHz, FOV of 24 cm, in-plane matrix of 512×384, and FA of 25°. Three slabs with 36 1mm-thick slices and 12 slices of overlap were determined to best minimize signal saturation for the TOF images while maintaining a large enough 3D volume for adequate SNR of the later echoes. The acquisition was accelerated in phase encoding direction using ARC with a acceleration factor of 3 and 16 autocalibrating lines, for total acquisition time of 11:05 minutes. *Image Reconstruction:* Partially-acquired k-space echoes were first reconstructed using POCS[6] before subsequent image reconstruction. TOF angiography was generated by maximum intensity projection (maxIP) of images from the first echo. Standard SWI post-processing was performed on each subsequent echo individually, and on a composite image whereby both magnitude images and phase masks from the last 3 echoes were first averaged to improve SNR prior to the multiplication between the two. All SWI images were minimum intensity projected though 8mm thickness to visualize CMBs and veins. *Validation:* The sequence was evaluated on a volunteer and two patients using GE 7T scanner with a 32-channel head coil. Both patients had multiple confirmed CBMs due to prior radiation therapy of a resected glioma. For the volunteer, previously optimized single-echo TOF and SWI sequences with the same acceleration, FOV, image matrix, and similar acquisition parameters (TOF: TE/TR/TA/FA/BW =2.7ms/30msec/6:40min/25°/41.76kHz, 3 slabs with 30 1mm-thick slices and 6 overlaps, 65% partial echo sampling; SWI: TE/TR/TA/FA/BW=16ms/ 50ms/5:20min/25°/15.63kHz, 1 slab with 40 2mm-thick slices, full echo) were also acquired for comparison. All three scans were each acquired two times on the volunteer in order to compare CNR between sequences. Noise within ROIs of background tissue on the TOF and white matter on SWI was calculated using the root-mean-square of the difference in voxel intensity between two successive identical acquisitions. CNR of arteries on the maxIP TOF and veins on the minIP SWI compared to background tissue was then calculated as the difference in mean values between ROIs divided by the noise.

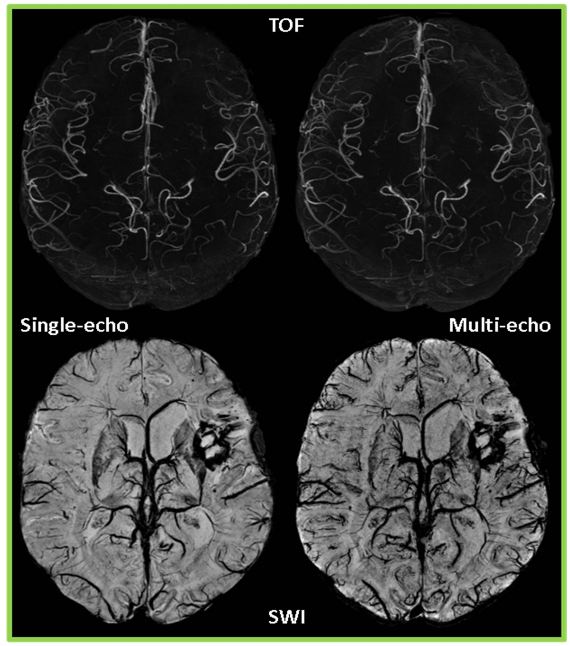

Fig 1. MaxIP TOF images and minIP SWI images acquired from a patient with radiation-induced CMBs with both single- and multi-echo sequences.

Results: Table 1 lists CNRs calculated for different acquisitions from the volunteer. CNRs of the multi-echo sequence were only 15% and 36.8% lower than the optimized single-echo sequences, for the TOF and combined SWI respectively. The combined SWI CNRs was approximately 1.5 times higher than the SWI CNR of any individual echo. However, the degraded CNR of the multi-echo acquisition did not compromise the conspicuity of arteries, veins and CMBs as shown in Fig.1. Visually, the images had only slightly worse background suppression on the TOF image and increased noise level on SWI. The SWI from the multi-echo sequence had the added advantage of visualizing smaller CMBs and veins not seen in the single-echo scan, as shown in Fig.2, due to the heightened slice resolution. The multi-echo SWI sequence was able to detect 24 CMBs from two patients in total compared to 19 with the single-echo sequence.

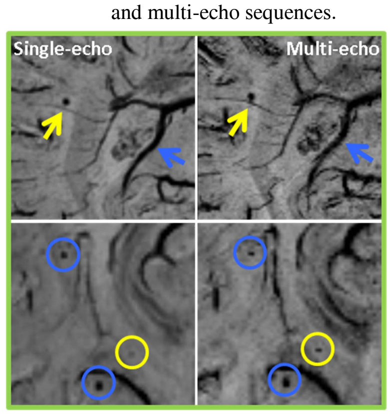

Fig 2. SWI images from patients. *Top row*: Single-echo SWI better delineates larger veins (blue arrows) due to its overall high CNR, while multi-echo SWI better illustrates smaller veins and their proximity to CMBs (yellow arrows) because of higher slice resolution. *Bottom row*: Two CMBs (blue circles) are visualized on both images, but one small CMB can only be seen on multi-echo SWI (yellow circles).

Discussion: Implementation a multi-echo sequence requires the careful selection of imaging parameters to achieve adequate background suppression on TOF MRI and reasonable CNR preservation on SWI. The required longer TR and thicker slabs for the SWI result in reduced background suppression and lower CNRs for the TOF images, while the multi-slab, partial echo acquisition with thinner slices necessary for TOF degrade the quality of SWI images. Despite these tradeoffs, our results have shown that the parameters we selected in combination with modified SWI processing of the later echoes were able to preserve the quality of both TOF and SWI images with good contrast. The thinner slice thickness achieved with the multi-echo SWI, also facilitated CMB detection compared to a single-echo SWI acquired with similar acquisition time and coverage.

Conclusion: Simultaneously acquired 3D TOF and SWI at 7T from the implemented multi-echo sequence achieved an image quality comparable to that of each individual single-echo sequence for intracranial arteries, veins and radiation-induced CMBs. The additional flexibility in SWI processing with multiple echoes allowed for thinner slices, which not only improved CMB detection, but also the contrast of smaller veins. Ultimately, this multi-echo acquisition will allow the merging of arteries, veins, and microbleeds on one image to facilitate quantification of metrics that reflect the interaction among these structures in order to characterize the mechanism of radiation-induced vascular injury.

References: 1. Lupo JM et al, *Int J Radiat Oncol Biol Phys* 2012; 82:493-500. 2. Haacke EM et al., *MRM* 2004;52:612-618. 3. Nishimura DG et al., *MRM* 1990;14:194-201. 4. DU YP et al., *MRM* 2008;59:954-958. 5. Deistung A, *JMRI* 2009;29:1478-1484. 6. Haacke EM, *JMR* 1991;92:126–145.

Acknowledgement: This work was supported by UC Discovery grant ITL-BIO04-10148